



# Portable NIR Applied to the Evaluation of Resin, Glue and Agglutinant used in Canvas Paintings

## NIR Portátil Aplicado à Avaliação de Resina, Cola e Aglutinante usados em Pinturas sobre Tela

Fábio Luiz Melquiades<sup>1</sup> , Rafael Molari<sup>1</sup> , Carlos Roberto Appoloni<sup>1</sup>

Received: January 14, 2025

Received in revised form: April 30, 2025

Accepted: June 30, 2025

Available online: July 25, 2025

### ABSTRACT

The aim of this work was to study various compounds commonly used in painting canvases by employing portable near-infrared spectroscopy (portable NIR) and to discriminate the compounds through exploratory statistical analysis of the spectra data. To this end, a painting specifically created for archaeometric analysis was examined. Two portable spectrometers with complementary wavelength ranges were combined for the measurements, one operating from 900 to 1700 nm ( $11100 - 5880 \text{ cm}^{-1}$ ) and the other from 1350 to 2150 nm ( $7400 - 4650 \text{ cm}^{-1}$ ). Portable NIR spectrometry identified characteristic spectral bands for each class of compound: waxes, binders, organic resins, and acrylic resins. Applying exploratory statistics via principal component analysis (PCA) allowed for material differentiation. This study demonstrated that combining NIR spectroscopy and PCA is a versatile tool for achieving consistent results in this application.

**keywords** archaeometry, canvas painting, NIR spectroscopy, exploratory analysis

### RESUMO

Este trabalho teve como objetivo estudar diferentes compostos comumente usados na pintura de telas empregando a espectroscopia no infravermelho próximo com o uso de equipamentos portáteis (NIR portátil) e através dos espectros, discriminá-los usando análise estatística exploratória. Para essa finalidade, foi avaliada uma pintura preparada especificamente para estudos arqueométricos. Dois espectrômetros portáteis com faixas de comprimento de onda complementares foram combinados para as medições, sendo um operando de 900 a 1700 nm ( $11100 - 5880 \text{ cm}^{-1}$ ) e o outro de 1350 a 2150 nm ( $7400 - 4650 \text{ cm}^{-1}$ ). A espectrometria NIR portátil permitiu a identificação de espectros com bandas características de cada classe dos compostos estudados: cera, aglutinantes, resinas orgânicas e resinas acrílicas. Com a aplicação de estatística exploratória através da análise de componentes principais (PCA) foi possível diferenciar os materiais. Foi constatado que a combinação de espectroscopia NIR e PCA se adequou como uma ferramenta versátil para alcançar resultados consistentes na aplicação desejada.

**palavras-chave** arqueometria, pintura em cavalete, espectroscopia NIR, análise exploratória

<sup>1</sup>Prof. Dr., Applied Nuclear Physics Laboratory, State University of Londrina (UEL), Londrina, PR, Brazil.  
[fmelquiades@uel.br](mailto:fmelquiades@uel.br), [rmolari@uel.br](mailto:rmolari@uel.br), [appoloni@uel.br](mailto:appoloni@uel.br)

## Introduction

A canvas painting has different layers depending on the technique and particular effects the artist intends to impress. In a simplified description, a canvas structure is composed of a support (wood, fabric canvas), a preparation layer (glue, gypsum, etc), a pictorial layer (paint layers) and a coating layer (glaze and varnish). An artist employs different ingredients in each layer to produce a work of art. Considering that, the focus of this paper is to provide a technical contribution in the evaluation of some components from products used in the preparation layer and coating layer such as animal glues, wax, organic resins, acrylic resins, and agglutinants (Cabral, 1995; Colombini et al., 2022).

Conservation and restoration of a canvas require knowledge about the materials employed by the artist in its production. The raw materials, agglutinants, binders and pigments characterizations are of fundamental importance. Archaeometric methods based on spectroscopy techniques are non-destructive and recommended to be part of an initial canvas examination prior to micro-sample extraction. There are some options with X-ray, ultraviolet, visible and infrared radiation depending on the analyst's interest or on the questions to be solved.

To evaluate binders based on organic resins (alkyd and vinyl), acrylic resins, lipids and proteins, the recommended fingerprint method is the near and mid-infrared spectroscopy. The attractive features of near-infrared spectroscopy (NIR) in reflectance mode such as rapidity, portability, non-invasive and contactless analysis, and cost-effective method have increased the interest towards its application in archaeometry studies Vagnini et al. (2009). Molecular and structural information about the sample surface is obtained from electronic and vibrational transitions detected in the analysis. NIR spectrometry comprises the range from 900 to 2500 nm (11100 to 4000  $\text{cm}^{-1}$ ). In this range, the spectrometer outputs are, in general, spectral bands from NH, CH, OH and CO combination and their overtone modes (Dooley et al., 2017; Weyer, 1985), which are related to proteins, lipids, organic resins and acrylic resins (Brunetti et al., 2016). The challenge is to interpret the combination of bands that characterize a family of binders or a specific compound.

Therefore, to contribute to the understanding and the characterization of binders applied in canvas painting, the aim of this work was to study, technically, different compounds commonly used in canvas painting using portable near-infrared spectroscopy (portable NIR) and, through the spectra, to discriminate them using exploratory statistical analysis. The measurements with portable devices were performed on several known products applied over a mimetic canvas prepared specifically for archaeometric research purposes.

## Material and methods





















In this study, a mockup painting, illustrated in Figure 1, prepared specifically for archaeometric studies was evaluated. The binder and pigments employed in the mockup canvas were commercial ingredients with known provenance, and some of them had known composition. It was previously evaluated by X-ray spectrometric methods for inorganic characterization of the pigments (Appoloni et al., 2023). The mockup had strips on the borders with individual materials, metal foils, antique pigments and modern pigments. The central area contained several combinations of the individual compounds used in the rectangles on the strips. The mockup was not subject to any type of aging or treatment. The strips on the left and upper sides of the mockup painting had no underlayer preparation and were divided into 44 rectangles. In the present study, the strip on the left side, comprising the chips from 1 to 19 and 24, were evaluated. The chips had 1 cm  $\times$  2 cm dimensions approximately. Each one of them had solely one material applied directly on the canvas without any kind of preparation. They were classified as agglutinant, wax, organic resin and polymeric resin, as described in Table 1.

Two portable spectrometers with complementary wavelength ranges were combined for the measurements: the NIR-S-G1 (900 – 1700 nm or 11100 – 5880  $\text{cm}^{-1}$ ) and the NIR-M-R11 (1350 – 2150 nm or 7400 – 4650  $\text{cm}^{-1}$ ) (InnoSpectra Co., Hsinchu, Taiwan), both with a DLP micromirror array, a single InGaAs detector, with 12 nm resolution. The measurements were performed directly on the chips containing the different compounds. The spectrometers have a protective glass window and each one of them was positioned over each rectangle at 1 mm distance. The spectrometers were configured to register 30 scans in 20 s in each round and the average spectrum is registered. All the points were measured in duplicate and an average spectrum was computed for analysis.

**Figure 1** - The complete view of the mockup canvas painting.



**Table 1** Binder types and visual chips representation.

No.	Binder	Binder Type	Chips	No.	Binder	Binder Type	Chips
1	rabbit skin glue	agglutinant		11	methacrylate	acrylic resin	
2	bone glue	agglutinant		12	acrylic resin	acrylic resin	
3	gum arabic crystals	agglutinant		13	vinyl acetate	acrylic resin	
4	microcrystalline wax	wax		14	polyamide	acrylic resin	
5	beeswax	wax		15	damar resin	organic resin	
6	carnauba wax	wax		16	casein	agglutinant	
7	copal resin	organic resin		17	egg white	agglutinant	
8	mastique resin	organic resin		18	egg yolk	agglutinant	
9	lacca gum	agglutinant		19	linseed oil	agglutinant	
10	polyvinyl acetate	acrylic resin		24	rosin resin	organic resin	

The acquired raw spectra were used in the exploratory analysis, which was performed using principal component analysis (PCA). Prior to the modeling, the following preprocessing sequences were applied: Multiplicative scatter correction + First derivative Savitz-Golay with second order polynomial and 15 window channels + Mean Center.

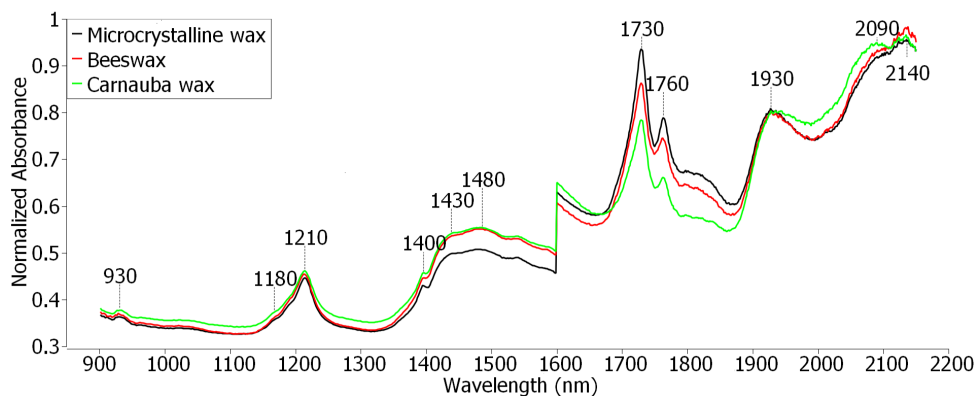
## Results and discussion

### Spectra interpretation

As mentioned, the objective of this study is to contribute to a technical evaluation of the binders commonly applied in canvas painting evaluating known ingredients using a portable NIR spectrometer. Some characteristic bands appeared in all the chips.

The bands from O-H bonding related to water are well defined around 1430 nm ( $6993\text{ cm}^{-1}$ ), 1480 nm ( $6757\text{ cm}^{-1}$ ) and 1930 nm ( $5181\text{ cm}^{-1}$ ) (Panero et al., 2018; Weyer, 1985), as observed in the spectra of Figure 2. In addition, the absorption band at 930 nm ( $10753\text{ cm}^{-1}$ ) could be associated with the C-O band of lipids/oil (Tsenkova et al., 1999).

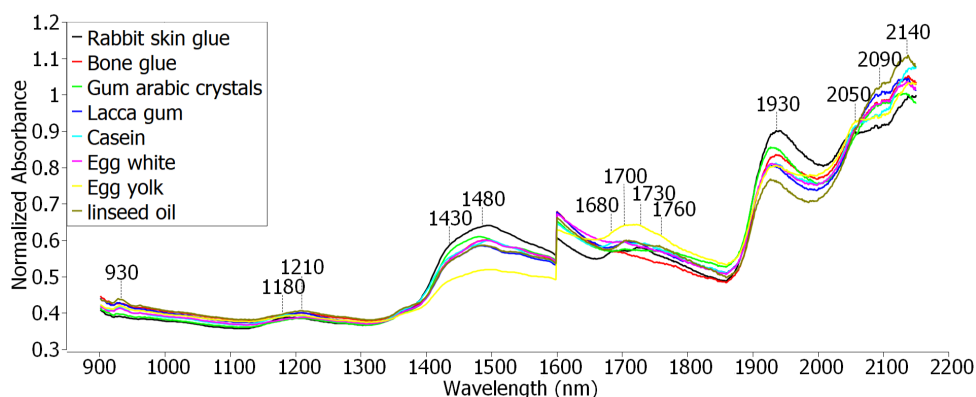
**Figure 2** - Wax samples spectra preprocessed with multiplicative scattering correction.



The wax samples were characterized through the characteristic absorptions of  $\text{CH}_2$  and  $\text{CH}$  combination bands and overtones at 1210 nm ( $8265\text{ cm}^{-1}$ ), 1730 nm ( $5780\text{ cm}^{-1}$ ) and 1760 nm ( $5682\text{ cm}^{-1}$ ) (Ciofini et al., 2016; Furukawa et al., 2002; Longoni et al., 2022; Vagnini et al., 2009) as illustrated in Figure 2. The band at 2140 nm ( $4673\text{ cm}^{-1}$ ) may be attributed to C-H deformation or  $\nu(\text{C-H})$  and  $\nu(\text{C=O})$  combination (Panero et al., 2018). Furthermore, the band at about 1180 nm ( $8475\text{ cm}^{-1}$ ) may be related to C-O (Invernizzi et al., 2018), and around at 1400 nm ( $7143\text{ cm}^{-1}$ ) there is a band from the O-H first overtone.

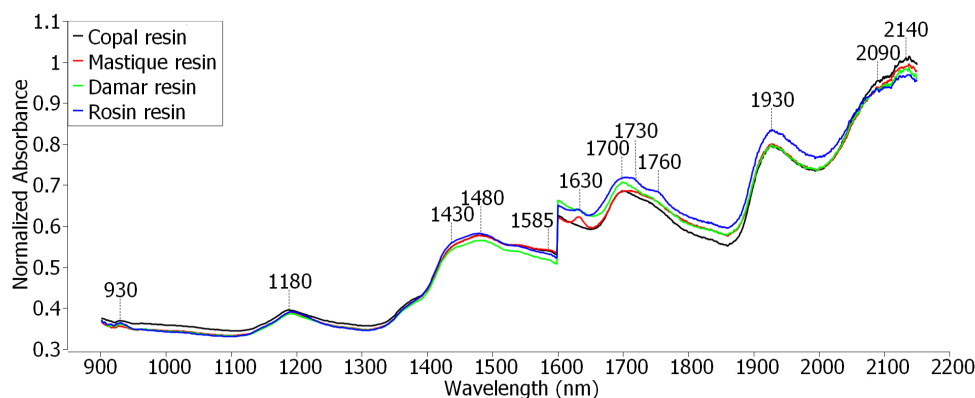
Slight differences in the agglutinant samples are noted from 1650 to 1800 nm ( $6060$  to  $5555\text{ cm}^{-1}$ ) as presented in Figure 3. Casein presents a characteristic band at 1680 nm ( $5917\text{ cm}^{-1}$ ). Arabic gum and linseed oil have a band at 1760 nm ( $5682\text{ cm}^{-1}$ ) from  $\text{CH}_2$  first overtone. Lacca gum and egg yolk have bands at 1700 nm ( $5930\text{ cm}^{-1}$ ) and 1730 nm ( $5780\text{ cm}^{-1}$ ) related to the 1st overtone  $\text{CH}_2$  (Furukawa et al., 2002; Vagnini et al., 2009). The band at about 1180 nm can also be related to C-O. At 1210 nm ( $8265\text{ cm}^{-1}$ ) a band is observed, referring to the 2nd harmonic of  $\nu(\text{C-H})$ . The band at 2050 nm ( $4878\text{ cm}^{-1}$ ) may be ascribed to  $\nu(\text{NH}) + \delta(\text{NH})$  (Vagnini et al., 2009), and the band around 2140 nm ( $4673\text{ cm}^{-1}$ ) may characterize the C-H deformation or  $\nu(\text{C-H})$  and  $\nu(\text{C=O})$  combination (Panero et al., 2018).

**Figure 3** - Agglutinant samples spectra preprocessed with multiplicative scattering correction.

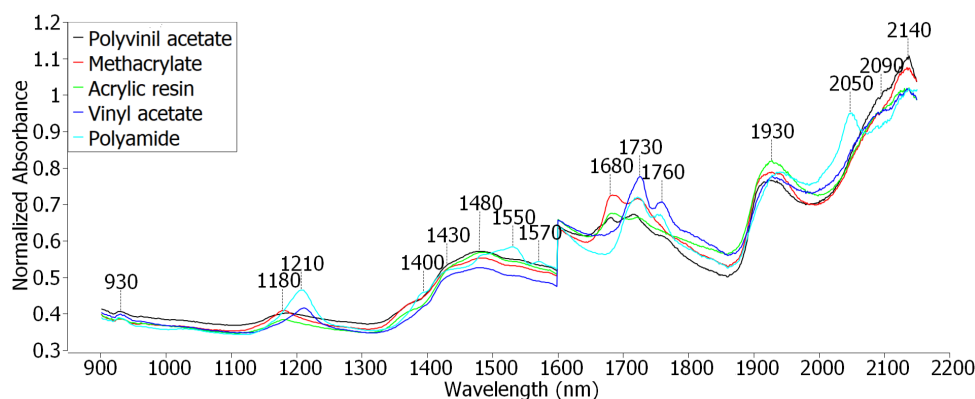


Organic resin presented bands at 1180 nm ( $8475\text{ cm}^{-1}$ ) due to the second overtone of  $\text{CH}_2$ , see Figure 4. There is an indication of a band at 1700 nm ( $5882\text{ cm}^{-1}$ ) related to the first  $\text{CH}_2$  overtone. The bands at 1730 nm ( $5780\text{ cm}^{-1}$ ) and 2140 nm ( $4673\text{ cm}^{-1}$ ) are due to C-O and  $\text{CH}_2$  bonds (Longoni et al., 2022). The mastic resin was the only one with a pronounced band at 1630 nm ( $6135\text{ cm}^{-1}$ ) due to the  $\text{CH}_2$  first overtone (Vagnini et al., 2009). In addition, the band at 1760 nm ( $5682\text{ cm}^{-1}$ ) is also related to the  $\text{CH}_2$  first overtone.



**Figure 4** - Organic resin samples spectra preprocessed with multiplicative scattering correction.

Acrylic resin set has 5 different samples as illustrated in Figure 5. Polyamide and vinyl acetate are characterized by 1210, 1730 and 1760 nm ( $8265$ ,  $5780$ ,  $5682$   $\text{cm}^{-1}$ ) bands corresponding to  $\text{CH}_2$  absorption and  $\text{CH}$  combination bands and overtones (Panero et al., 2018). However, polyamide has an extra band at 2050 nm which corresponds to one of the  $\text{NH}$  bands from amide (Unger et al., 2011) and clearly differentiates this sample from the others. Vinyl acetate has the highest bands at 1730 and 1760 nm ( $5780$  and  $5682$   $\text{cm}^{-1}$ ). The bands around 1550 and 1570 nm ( $6452$  and  $6370$   $\text{cm}^{-1}$ ) may be related to the vibrational  $\text{N-H}$  bands, and around 2140 nm ( $4673$   $\text{cm}^{-1}$ ), the observed band may be characterized by the  $\text{C-H}$  deformation or  $\nu(\text{C-H})$  and  $\nu(\text{C=O})$  combination (Panero et al., 2018). Around 1400 nm ( $7143$   $\text{cm}^{-1}$ ) there is a band from the  $\text{O-H}$  first overtone (Tsenkova et al., 1999). Finally, according to (Rufino & Monteiro, 2003), the band close to 1680 nm ( $5952$   $\text{cm}^{-1}$ ) may be related to the  $\text{C-H/CH}_2$ ,  $\text{CH}_3$  stretch.

**Figure 5** - Acrylic resin samples spectra preprocessed with multiplicative scattering correction.

In general terms, the spectrometers employed were able to identify the different groups of elements. Table 2 presents a synthesis of the bands identified by the portable instrument that characterize each chip ingredient. Some important differences can be noticed. For instance, the 2050 nm band is present only in the spectra of rabbit skin and bone glues, casein, egg yolk, and polyamide; the 1585 nm band is present only in the spectra of Copal, Damar, mastic, and Rosin resins; the 1630 nm band is present only in the spectrum of mastic resin; the 1550 and 1570 nm bands are present only in the spectrum of polyamide; the 1400 nm band is present only in the spectra of the three waxes and polyamide.

### Exploratory data analysis

The PCA with all the spectra considering 4 PCs accomplished 86.5% of explained variance. However, the first two PCs plot, which explains 70.5% of the data variance, represents the global discrimination reached by this analysis.

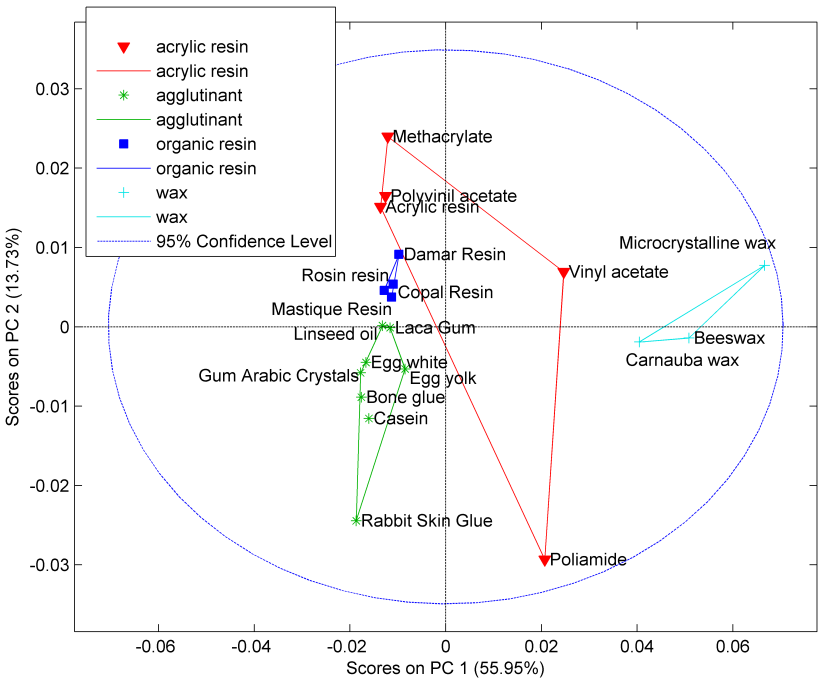
In a general view, the score plot, Figure 6, shows that the wax samples are well separated in PC1 positive direction, acrylic resin samples are spread along PC2 direction due to their multiple bands at 1600, 1650 and 2060 nm. Polyamide is the one with the lower intensity of these bands and because of that it appears in PC2 negative direction. The organic resin samples form a concise grouping in the PC1 negative direction.

**Table 2** - Synthesis of the characteristic bands of each material/ingredient. The bands from water (1430, 1480, and 1930 nm) were not included because they are common to all measurements.

Material	Bands (nm)												
	1180	1210	1400	1550	1570	1585	1630	1680	1700	1730	1760	2050	2090
Microcrystalline wax	x	x	x	—	—	—	—	—	—	x	x	—	x
Bees wax	x	x	x	—	—	—	—	—	—	x	x	—	x
Carnauba wax	x	x	x	—	—	—	—	—	—	x	x	—	x
Rabbit skin glue	x	x	—	—	—	—	—	—	—	x	—	x	x
Bone glue	—	x	—	—	—	—	—	—	—	—	—	x	x
Gum arabic crystals	—	x	—	—	—	—	—	—	x	—	x	—	x
Lacca gum	—	x	—	—	—	—	—	—	x	x	—	—	x
Casein	x	x	—	—	—	—	—	x	—	—	—	x	—
Egg white	—	x	—	—	—	—	—	—	x	—	—	—	x
Egg yolk	x	x	—	—	—	—	—	—	x	x	—	x	—
Linseed oil	—	x	—	—	—	—	—	—	x	—	x	—	x
Copal resin	x	—	—	—	—	x	—	—	x	x	x	—	x
Mastic resin	x	—	—	—	—	x	x	—	x	x	x	—	x
Damar resin	x	—	—	—	—	x	—	—	x	x	x	—	x
Rosin resin	x	—	—	—	—	x	—	—	x	x	x	—	x
Polyvinyl acetate	x	—	—	—	—	—	—	x	—	x	—	—	x
Methacrylate	x	—	—	—	—	—	—	x	—	x	—	—	—
Acrylic resin	x	—	—	—	—	—	—	x	—	x	—	—	x
Vinyl acetate	x	x	—	—	—	—	—	—	—	x	x	—	x
Polyamide	—	x	x	x	x	—	—	—	—	x	x	x	—

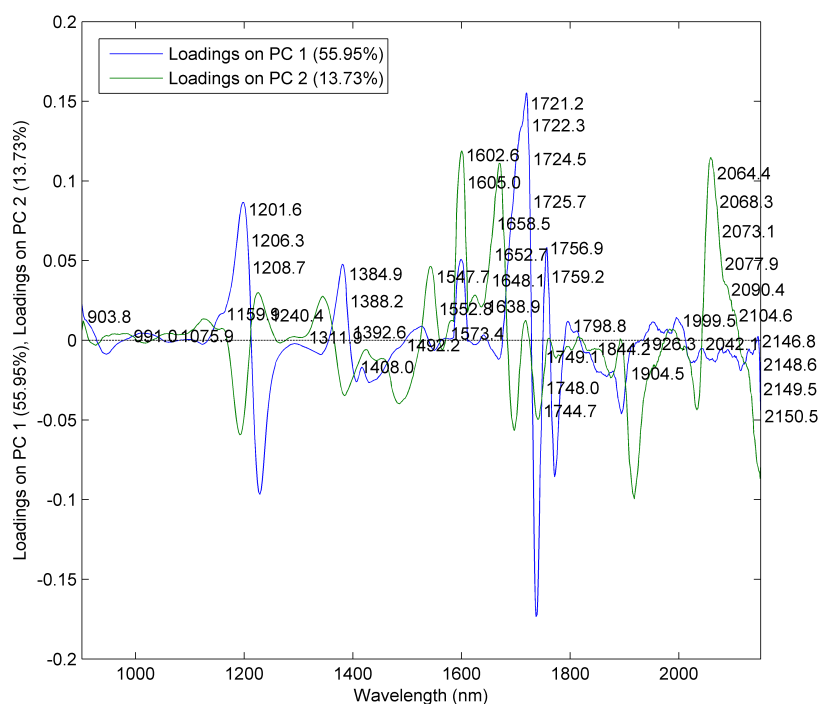
Note: “x” indicates the presence of a band, and “—” indicates the absence of a band.

**Figure 6** - Scores plot.



The proteinaceous tempera, i.e., the agglutinants, are at the third quadrant of the score plot and have an influence of PC1 and PC2 negative direction, specifically 1740, 1905 and 1200 bands. The wax samples are the most prominent group in the score plot. It is positioned in the extreme positive direction of PC1, separated due to the higher intensity in bands of 1720 nm and 1200 nm according to the loadings plot presented in Figure 7.

**Figure 7** - Loadings plot.



## Conclusions

Portable NIR spectrometry enabled the differentiation between the binder families evaluated, i.e., Wax, Agglutinants, Organic Resin and Acrylic Resin. The characteristic bands of each class of organic compounds were identified, and the PCA allowed their discrimination. The portable NIR used in this study is an effective low-cost tool for the characterization of molecular compounds in canvas paintings and may be a complementary tool to X-ray fluorescence, which is widely used in archaeometry for the determination of inorganic components, especially pigments.

## Author contributions

**F. L. Melquiades** participated in conceptualization, data curation, formal analysis, funding acquisition, investigation, methodology, supervision, and writing – original draft. **R. Molari** participated in formal analysis, methodology, validation, and visualization. **C. R. Appoloni** participated in supervision, validation, and writing – review and editing.

## Conflicts of interest

The authors declare no conflict of interest.

## Acknowledgements

The authors acknowledge Dr. Márcia Rizzo for the mimetic preparation. Also the support from CNPq (grant number 306309/2023-8 and project number: 404214/2021-5), INCT-FNA (grant number 464898/2014-5).

## References

- Appoloni, C. R., Lopes, F., Rizzutto, M. d. A., Neiva, A. C., Ikeoka, R. A., & Rizzo, M. d. M. (2023). Pixe and pxf comparison analysis of a mockup canvas painting. *Semina: Ciências Exatas e Tecnológicas*, 44, e47604. <https://doi.org/10.5433/1679-0375.2023.v44.47604>
- Brunetti, B., Miliani, C., Rosi, F., Doherty, B., Monico, L., Romani, A., & Sgamellotti, A. (2016). Non-invasive investigations of paintings by portable instrumentation: The MOLAB experience. *Topics in Current Chemistry*, 374(10), 1–35. <https://doi.org/10.1007/s41061-015-0008-9>
- Cabral, J. M. P. (1995). Exame científico de pinturas de cavalete. *Colóquio / Ciências*, 16, 60–83.
- Ciofini, D., Striova, J., Camaiti, M., & Siano, S. (2016). Photo-oxidative kinetics of solvent and oil-based terpenoid varnishes. *Polymer Degradation and Stability*, 123, 47–61. <https://doi.org/10.1016/j.polymdegradstab.2015.11.002>
- Colombini, M. P., Degano, I., & Nevin, A. (2022). Analytical approaches to the analysis of paintings: An overview of methods and materials. In M. P. Colombini, I. Degano, & A. Nevin (Eds.), *Analytical Chemistry for the Study of Paintings and the Detection of Forgeries* (pp. 95–111). Springer. [https://doi.org/10.1007/978-3-030-86865-9\\_3](https://doi.org/10.1007/978-3-030-86865-9_3)
- Dooley, K. A., Coddington, J., Krueger, J., Conover, D. M., Loew, M., & Delaney, J. K. (2017). Standoff chemical imaging finds evidence for jackson pollock's selective use of alkyd and oil binding media in a famous 'drip' painting. *Analytical Methods*, 9(1), 28–37. <https://doi.org/10.1039/C6AY01795A>
- Furukawa, T., Kita, Y., Sasao, S., Matsukawa, K., Watari, M., Šašić, S., Siesler, H. W., & Ozaki, Y. (2002). On-line monitoring of melt-extrusion transesterification of ethylene vinylacetate copolymers by near infrared spectroscopy and chemometrics. *Journal of Near Infrared Spectroscopy*, 10(3), 195–202. <https://doi.org/10.1255/jnirs.335>
- Invernizzi, C., Rovetta, T., Licchelli, M., & Malagodi, M. (2018). Mid and Near-Infrared Reflection Spectral Database of Natural Organic Materials in the Cultural Heritage Field. *International Journal of Analytical Chemistry*, 2018(1), 1–16. <https://doi.org/10.1155/2018/7823248>
- Longoni, M., Genova, B., Marzanni, A., Melfi, D., Beccaria, C., & Bruni, S. (2022). Ft-nir spectroscopy for the non-invasive study of binders and multi-layered structures in ancient paintings: Artworks of the lombard renaissance as case studies. *Sensors*, 22(5), 2052. <https://doi.org/10.3390/s22052052>
- Panero, J. S., Silva, H. E. B. d., Panero, P. S., Smiderle, O. J., Panero, F. S., Faria, F. S. E. D. V., & Rodriguez, A. F. R. (2018). Separation of cultivars of soybeans by chemometric methods using near infrared spectroscopy. *Journal of Agricultural Science*, 10(4), 351. <https://doi.org/10.5539/jas.v10n4p351>
- Rufino, E. S., & Monteiro, E. E. C. (2003). Infrared study on methyl methacrylate–methacrylic acid copolymers and their sodium salts. *Polymer*, 44(23), 7189–7198. <https://doi.org/10.1016/j.polymer.2003.08.041>
- Tsenkova, R., Atanassova, S., Toyoda, K., Ozaki, Y., Itoh, K., & Fearn, T. (1999). Near-infrared spectroscopy for dairy management: Measurement of unhomogenized milk composition. *Journal of Dairy Science*, 82(11), 2344–2351. [https://doi.org/10.3168/jds.S0022-0302\(99\)75484-6](https://doi.org/10.3168/jds.S0022-0302(99)75484-6)
- Unger, M., Ozaki, Y., & Siesler, H. W. (2011). Variable-temperature fourier transform near-infrared (ft-nir) imaging spectroscopy of the diffusion process of butanol(od) into polyamide 11. *Applied Spectroscopy*, 65(9), 1051–1055. <https://doi.org/10.1366/11-06309>
- Vagnini, M., Miliani, C., Cartechini, L., Rocchi, P., Brunetti, B. G., & Sgamellotti, A. (2009). Ft-nir spectroscopy for non-invasive identification of natural polymers and resins in easel paintings. *Analytical and Bioanalytical Chemistry*, 395(7), 2107–2118. <https://doi.org/10.1007/s00216-009-3145-6>

Weyer, L. G. (1985). Near-infrared spectroscopy of organic substances. *Applied Spectroscopy Reviews*, 21(1–2), 1–43. <https://doi.org/10.1080/05704928508060427>